Geophysical Research Letters

RESEARCH LETTER
10.1029/2023GL107523

The Decreased Cloud Cover Dominated the Rapid Spring Temperature Rise in Arid Central Asia Over the Period 1980–2014

Gongxin Wang[1,2], Xiuliang Yuan[1,3], Changqing Jing[2], Rafiq Hamdi[1,4], Friday Uchenna Ochege[1], Ping Dong[2], Yuqing Shao[2], and Xueyan Qin[1,3]

[1]State Key Laboratory of Desert and Oasis Ecology, Xinjiang Institute of Ecology and Geography, Chinese Academy of Sciences, Urumqi, China, [2]College of Grassland Science, Xinjiang Agricultural University, Urumqi, China, [3]University of Chinese Academy of Sciences, Beijing, China, [4]Royal Meteorological Institute, Brussels, Belgium

Key Points:

- The rapid spring warming contributed most to the annual temperature increase in Central Asia (CA) among other seasons
- The rapid spring average temperature rise in arid CA was mainly driven by the decreased cloud cover
- The increase in sea level pressure led to the subsidence of vertical motion over CA and consequently the decreased cloud cover

Supporting Information:

Supporting Information may be found in the online version of this article.

Correspondence to:

X. Yuan and C. Jing,
yuanxiuliang@ms.xjb.ac.cn;
jingchangqing@126.com

Citation:

Wang, G., Yuan, X., Jing, C., Hamdi, R., Ochege, F. U., Dong, P., et al. (2024). The decreased cloud cover dominated the rapid spring temperature rise in arid Central Asia over the period 1980–2014. *Geophysical Research Letters*, *51*, e2023GL107523. https://doi.org/10.1029/2023GL107523

Received 26 NOV 2023
Accepted 7 JAN 2024

Author Contributions:

Conceptualization: Xiuliang Yuan, Changqing Jing
Formal analysis: Gongxin Wang
Funding acquisition: Xiuliang Yuan, Changqing Jing
Supervision: Xiuliang Yuan, Changqing Jing
Visualization: Gongxin Wang, Yuqing Shao
Writing – original draft: Gongxin Wang, Xiuliang Yuan

Abstract Central Asia (CA) has experienced a faster temperature rise than the global land over the past decades. However, the role of regional/global drivers and their associated underlying biophysical mechanisms is poorly explored. Here, we combined observations and model simulations to show that the rapid warming in CA was overwhelmingly contributed by rapid spring warming (i.e., 49.23%). The decrease of cloud cover (CLD) was the main driver of spring warming in CA, leading to the surface receiving more solar radiation, consequently heating the surface air temperature, and contributing almost 40.79% to the spring warming. Besides, the strengthening of sea level pressure states results in continuous subsidence of vertical motion over CA, which was unfavorable for cloud formation. Our study will deepen our understanding of the climate evolution in the arid CA.

Plain Language Summary Central Asia (CA) has experienced a faster temperature rise than the global land over the past decades, which has brought unprecedented challenges to the survival and flourishing of life. The role of drivers and their associated underlying biophysical mechanisms is explored here. We conclude that the temperature increase in CA is overwhelmingly contributed by rapid warming in spring (i.e., 49.23%), and the rapidly increasing trend will continue till the end of this century. The decrease of cloud cover (CLD) was the main driver of spring warming in CA, leading to the surface receiving more solar radiation, and consequently heating the surface air temperature, contributing almost 40.79% to the spring warming. Besides, the strengthening of sea level pressure states results in subsidence of vertical motion over CA, which was unfavorable for cloud formation.

1. Introduction

Global warming has resulted in a rapid temperature rise over the past 30 years, at a rate of at least 0.2°C per decade (Fan et al., 2020; Stocker et al., 2014). This has profoundly impacted the global hydrological cycle (Hansen et al., 2010; Zheng et al., 2019), food production (Barrios et al., 2008), natural disasters (Mori et al., 2021), as well as socio-economic development (Diffenbaugh & Burke, 2019). Therefore, investigating the spatiotemporal trends in temperature change and quantifying the primary causes of warming is of great significance for predicting climate change and formulating the necessary adaptation measures for the future (Fan et al., 2020).

Central Asia (CA) is one of the driest regions in the world, characterized by its distance from the ocean, and consequently, scarce precipitation and sparse vegetation, whose ecosystems are particularly sensitive and vulnerable to climate warming (T. Chen et al., 2019). The CA has undergone rapid warming (F. Chen et al., 2009; Z. Hu et al., 2014) over the past century, faster than the global land average (Z. Chen et al., 2023; Fan et al., 2020) and other regions, such as South America, Australia and China (Fan et al., 2020; Q. Li et al., 2011). Furthermore, the temperature increase exhibits seasonal patterns, with certain studies suggesting a more rapid rate of warming in spring (Z. Hu et al., 2014; Xu et al., 2015), while in other studies, winter was found to have the biggest contributions to the annual warming (Huang et al., 2005; Peng et al., 2019; Trenberth & Josey, 2007). The discrepancies in conclusions may arise from divergent study periods and climate data sets utilized. Therefore, there is a need to quantify the relative contributions of different seasons to the annual mean temperature variations.

Writing – review & editing: Xiuliang Yuan, Changqing Jing, Rafiq Hamdi, Friday Uchenna Ochege, Ping Dong, Xueyan Qin

Temperature variations are generally driven by various factors, such as human activities (Peng et al., 2019), atmospheric circulation (H. Li & Fan, 2022), elevation (Dong et al., 2015), latitude (Revadekar et al., 2013), as well as urban morphology (Guo et al., 2020). By influencing various atmospheric circulation and energy exchange processes, the cloud (CLD) was also found to play a crucial role in regulating the climate (Shouguo et al., 2004). Specifically, dense cloud cover reflects incoming solar radiation and reduces absorption at the surface, having a cooling effect; meanwhile, clouds trap outgoing longwave radiation at night and keep the surface warm (G. Chen et al., 2022). Variations in cloud amount and vertical distribution impact atmospheric stability and temperature profiles by altering vertical motions and latent heating (Grant et al., 2022; C. Zhou et al., 2016). Furthermore, changes in cloudiness can also affect cyclonic activities and air mass exchanges by modifying the movements of air and water masses, leading to regional temperature anomalies (Bednorz et al., 2016). Besides, sea level pressure (SLP) variation is another important factor that influences temperature changes by controlling lower atmospheric circulations. For example, the Siberian high-pressure system has a significant impact on the temperature of the CA continent (Gong & Ho, 2002). The Arctic Oscillation is a leading indicator of winter SLP, accounting for 16% of the total variance in warm-season atmospheric circulation at the middle and high latitudes (Thompson & Wallace, 2000). Therefore, changes in CLD and atmospheric pressure systems have a certain impact on surface air temperatures, both of which can alter the local surface energy balance, leading to local temperature changes. However, the contributions of these factors to CA's temperature changes have not been thoroughly evaluated, which is helpful to give us a better understanding of temperature changes in CA in recent decades.

It is well-established that emissions of greenhouse gases, chiefly CO_2, represent the foremost contributor to global warming (Hájek et al., 2019). The resultant climate change stems from an alteration of the surface energy balance. However, this energy imbalance manifests unevenly in the horizontal dimension (Hansen et al., 2011; X. Hu et al., 2019), modulated primarily by heterogeneities in underlying surface characteristics (Duveiller et al., 2018; He et al., 2022). Such horizontal asymmetries may in turn impact local and regional climates (X. Hu et al., 2019; Marshall et al., 2015). In other words, while greenhouse gas forcing constitutes the primary mechanism, regional climate is also shaped by myriad other regional factors. Additional quantitative research is therefore imperative in arid regions. Comprehensive insights into spatiotemporal patterns and physical processes governing regional temperature change are crucial for improved projections and adaptation measures in these climate-sensitive zones.

To this end, we adopted Climate Research Unit (CRU) and Coupled Model Intercomparison Project phase 6 (CMIP6) temperature data sets to study temperature changes in CA over the past 35 years (1980–2014) and evaluated the contributions of different factors to the CA temperature. Finally, we attempted to identify the factors responsible for accelerating the warming trend in CA and explain why the spring warming rate is faster than that of global land.

2. Materials and Methods

2.1. Study Area

The CA region in this study is one of the driest regions in the world, consisting of Kazakhstan, Kyrgyzstan, Tajikistan, Turkmenistan, Uzbekistan, and Xinjiang Province, China. Geographically situated between 35°N–55°N and 50°E–95°E (Figure S1 in Supporting Information S1). CA has a typical temperate continental climate characterized by scarce precipitation, high evapotranspiration rates, and an arid environment (Bai et al., 2019; Jing & Li, 2016). Mean annual precipitation over the region is 211 mm and average temperature is 6.65°C (Deng & Chen, 2017). Over the past century, CA has experienced significant warming of 0.2–0.43°C per decade based on long-term observations (F. Chen et al., 2009; Z. Hu et al., 2014), with an increase of 1.6°C during the twentieth century (F. Chen et al., 2012). The primary sources of atmospheric moisture transport into CA are the North Atlantic, Northern Indian Ocean, Arctic Ocean, and Eurasian continent. Specifically, westerly circulation mainly influences inflow from the North Atlantic, while the monsoonal system brings moisture from the Northern Indian Ocean (Bothe et al., 2012; Sun & Wang, 2014). Topography and seasonality modulate moisture transport from the Eurasian interior.

2.2. Data

The surface air temperature (TMP), precipitation (PRE), and CLD were obtained from the CRU Time Series Data Version 4.06 (Harris et al., 2020). The CRU data sets were constructed by using angular-distance weighting

interpolation based on daily or sub-daily observations calculated by national meteorological agencies and other external proxies. The data sets have a very high level of accuracy and are commonly used to validate other data or directly used for scientific research purposes. Therefore, the monthly data sets with a resolution of 0.5° × 0.5°, spanning from 1901 to December 2020, were adopted in this study.

The monthly surface soil moisture (SM) data, spanning from 1980 to 2022 were obtained from the Global Land Evaporation Amsterdam Model (GLEAM) v3.7a at a 0.25° × 0.25° resolution (Martens et al., 2017). The GLEAM data set was produced based on a set of algorithms that estimate precipitation interception, infiltration of precipitation through the vertical soil profile, and components of terrestrial evapotranspiration.

The 500 hPa vertical velocity (VV) and SLP data sets were chosen to explore the mechanism-caused changes in CA temperature. These global atmospheric reanalysis data were jointly developed by the National Centers for Environmental Prediction (NCEP) and the National Center for Atmospheric Research, with a spatial resolution of 2.5° × 2.5° and covering the period from 1948 to 2018. We also used 500 hPa VV, SLP and surface solar radiation downwards (SSR) data sets of ERA5. These data are from the fifth generation of the European Center for Medium-Range Weather Forecasts atmospheric reanalysis data set, with a spatial resolution of 0.25° × 0.25° and covering the period from 1940 to 2022 (Table S1 in Supporting Information S1).

To test how the CA temperature changes in the future, the monthly surface air temperature data from 19 global climate models (GCMs) participating in the Scenario Model Intercomparison Project in the CMIP6 were used (Table S2 in Supporting Information S1). Three scenarios (SSP1-2.6, SSP2-4.5, and SSP5-8.5) were used for future projections from 2015 to 2100, providing full-range forcing targets similar in magnitude and distribution to those used in the Coupled Model intercomparison Project phase 5 RCPs (Gidden et al., 2019). The historical simulations from 1980 to 2014 were used to test the model performance.

All data sets were remapped into a common spatial resolution of 0.5 × 0.5° for analysis and comparison. In this study, we focused on both seasonal and annual (ANN) temperatures, with spring encompassing March–May (MAM); summer constituting June–August (JJA); autumn comprising September–November (SON); and winter consisting of December–February (DJF). Given that springtime was identified as the season exhibiting the greatest contribution to annual temperature changes (as will be elucidated in Section 3), our analysis of temperature variations was focused principally on the spring season.

2.3. Statistical Indicators

The recently introduced DISO index (i.e., Distance between Indices of Simulation and Observation) was applied to evaluate the performance of the CMIP6 models in capturing CA temperature changes (Z. Hu et al., 2022). The DISO index is advantaged by considering multiple statistical merits with different dimensions, such as absolute error (AE), correlation coefficient (r), and root-mean-square error (RMSE). Specifically, AE and RMSE were first rescaled as Normalized Mean Absolute Error (NAE) and Normalized Root Mean Square Error (NRMSE), respectively, by the min-max normalization to eliminate the influence of dimension. Obviously, the DISO value will be smallest when CRU temperature is compared to itself, with the values of $r = 1$, NAE = 0, and NRMSE = 0. The equation can be expressed as follows,

$$\mathrm{DISO}_i = \sqrt{(r_i - r_0)^2 + (\mathrm{NAE}_i - \mathrm{NAE}_0)^2 + (\mathrm{NRMSE}_i - \mathrm{NRMSE}_0)^2} \quad (1)$$

where $i = 0, 1, \ldots, n$, and n is the number of CMIP6 models; r represents the correlation coefficient; NAE is the Normalized Mean Absolute Error; and NRMSE is the Normalized Root Mean Square Error. When $i = 0$, $\mathrm{DISO}_0 = 0$, which indicates the distance between the observed values (OBS) and itself. The smaller the DISO value, the better the overall performance.

We utilized structural equation modeling (SEM) to examine the direction and magnitude of impacts of PRE, SSR, SM, and CLD on TMP (Grace, 2006). SEM allows to quantify the contributions of the independent variables (i.e., PRE, SSR, SM, and CLD) to the dependent variable (TMP). This approach can assess the strength of relationships among variables, and derive the direct, indirect, and total effects of the independent variables on the dependent variable. To evaluate the SEM established in this study, the fitness parameters such as the chi-square degree of freedom ratio (CMIN/DF) and the root mean square absolute error (RMSAE) were chosen. The smaller the value of CMIN/DF, the better fit of the model to the observed data. It ranges from 0 to 3, with values closer to 0 indicating better fit. Furthermore, the smaller the RMSAE, the smaller the difference between the model's

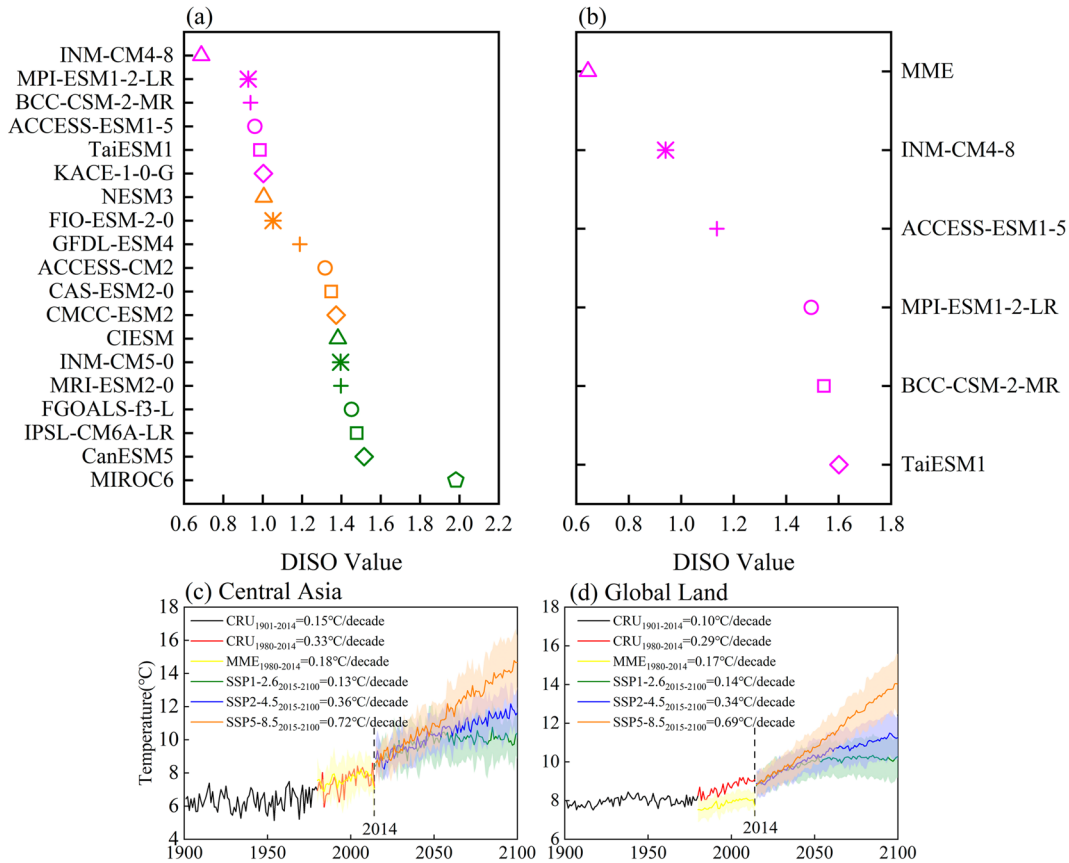

Figure 1. Annual changes of temperature. (a) The evaluation of 19 Coupled Model Intercomparison Project phase 6 (CMIP6) models in simulating temperature in Central Asia (CA); (b) Same as (a), but for the top five best-performing models and their ensemble mean value (multi-model ensemble [MME]); (c) The rate of warming in CA; (d) The rate of global warming over global land, and the shaded regions represent one standard deviation of the five models. The Distance between Indices of Simulation and Observation (DISO) value was used for the evaluation, calculated by the annual temperature between Climate Research Unit (CRU) data and the CMIP6 model from 1980 to 2014 in CA. The smaller the DISO value, the better the overall performance.

predictions and the observations, and the better the model performance. Besides, the linear regression method was used to fit the trend of temperature and its driving factors. And the Pearson's correlation (R) was used to analyze the relationship between them. The t-test was used to assess the statistical significance (p) of the trend and R.

3. Results

3.1. Temperature Change in Central Asia

CMIP6 models exhibited different capabilities in simulating TMP, as evidenced by the DISO value ranging from 0.69 to 1.98. By comparing to other CMIP6 models, the INM-CM4-8 model demonstrates the best simulation capability with the lowest DISO of 0.69, while the MIROC6 exhibits the poorest performance with the highest DISO of 1.98 (Figure 1a). Based on the DISO values, we selected the top five best-performing models (i.e., INM-CM4-8, MPI-ESM1-2-LR, BCC-CSM-2-MR, ACCESS-ESM1-5, and TaiESM1) and calculated the multi-model ensemble (MME) mean value to represent the simulated temperature for both historical and future periods. We found that the DISO value of the MME, 0.64, is the lowest among the five models (Figure 1b), confirming earlier studies that the MME performs better than individual models (G. Chen et al., 2022; Tian-Jun et al., 2021; Q. Zhang et al., 2023).

Over the period 1980–2014, the CRU reanalysis confirmed a faster warming trend in CA compared to the global land average, with values of 0.33 versus 0.29°C/decade, while a comparable warming trend was found by MME with values of 0.18 versus 0.17°C/decade (Figures 1c and 1d). The result was consistent, even when the study period was extended between 1901 and 2014 based on the CRU reanalysis, with values of 0.15 versus 0.10°C/decade.

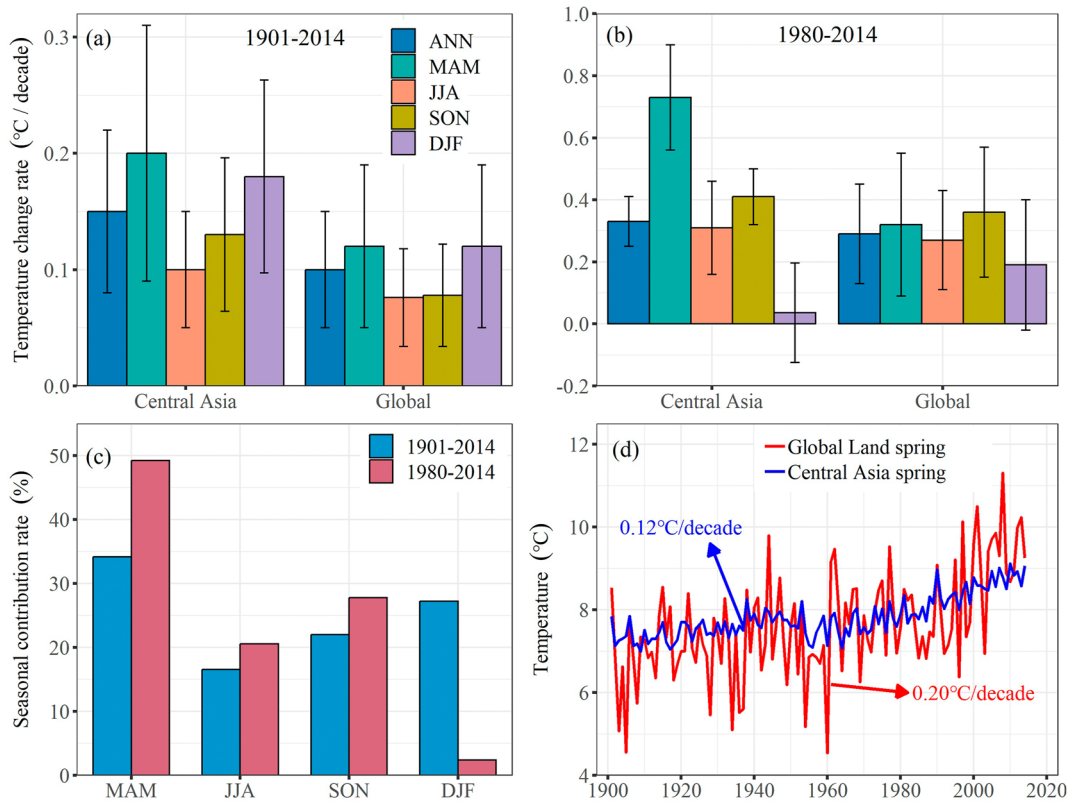

Figure 2. Seasonal patterns of temperature changes. (a) Seasonal temperature change rate in Central Asia (CA) and global land from 1901 to 2014; (b) Seasonal temperature change rate in CA and global land from 1980 to 2014; (c) Contribution rate of seasonal warming to the annual temperature trends in CA; (d) Temporal changes of spring temperature in CA and global land from 1980 to 2014. MAM, JJA, SON, and DJF denote spring, summer, autumn, and winter respectively. Error bars show 1 standard error in both (a) and (b).

However, the results show that the annual average temperature in CA rose at a higher rate during 1980–2014 than that over the past 114 years (1901–2014). The GCM simulations under both the medium-emission SSP2-4.5 and high-emission SSP5-8.5 scenarios further suggest that CA will likely experience an accelerated warming trend in the future (Figures 1c and 1d). Our findings suggest an uneven impact of climate change on different regions. This unevenness may lead to a more pressing and serious climate change challenge for the CA region.

Over 1901–2014, the warming rate across all seasons in CA outpaced the respective global averages, with the fastest temperature rise occurring in spring at 0.20 and 0.12°C/decade for both CA and the global land, respectively (Figures 2a and 2d). Correspondingly, from 1980 to 2014, spring persisted as the season with the highest warming in CA, but with an accelerated rate of 0.73°C/decade, nearly 3.5 times greater than the past century. For the global land, autumn replaced spring as the season with the fastest warming. On the contrary, the winter experienced a smallest warming trend in CA during the last 35 years from 0.18 to 0.04°C/decade (Figure 2b). Besides, the above results are also confirmed based on the spatial analyses that the spring and autumn seasons are the fastest warming globally and CA, respectively (Figures S2 and S3 in Supporting Information S1). Consequently, the contribution rate of spring warming to the annual mean temperature increased from 34.18% to 49.23%, while the winter sharply dropped from 16.58% to 2.42% (Figure 2c). Although both summer and autumn also exhibited accelerated warming in CA, their contributions to the annual mean rate remained stable at no more than 30%. These results indicate the dominance of spring warming in the overall CA temperature rise over the past 35 years.

3.2. Attribute of Factors to the Spring Warming in Central Asia

The Pearson correlation analysis was first used to identify potential factors (e.g., CLD, SSR, PRE, and SM) influencing CA spring temperature. Then, the contribution of these factors was further quantified by the SEM method. The results show that the spring temperature was significantly correlated to the CLD ($R = -0.63$, $p < 0.01$), while

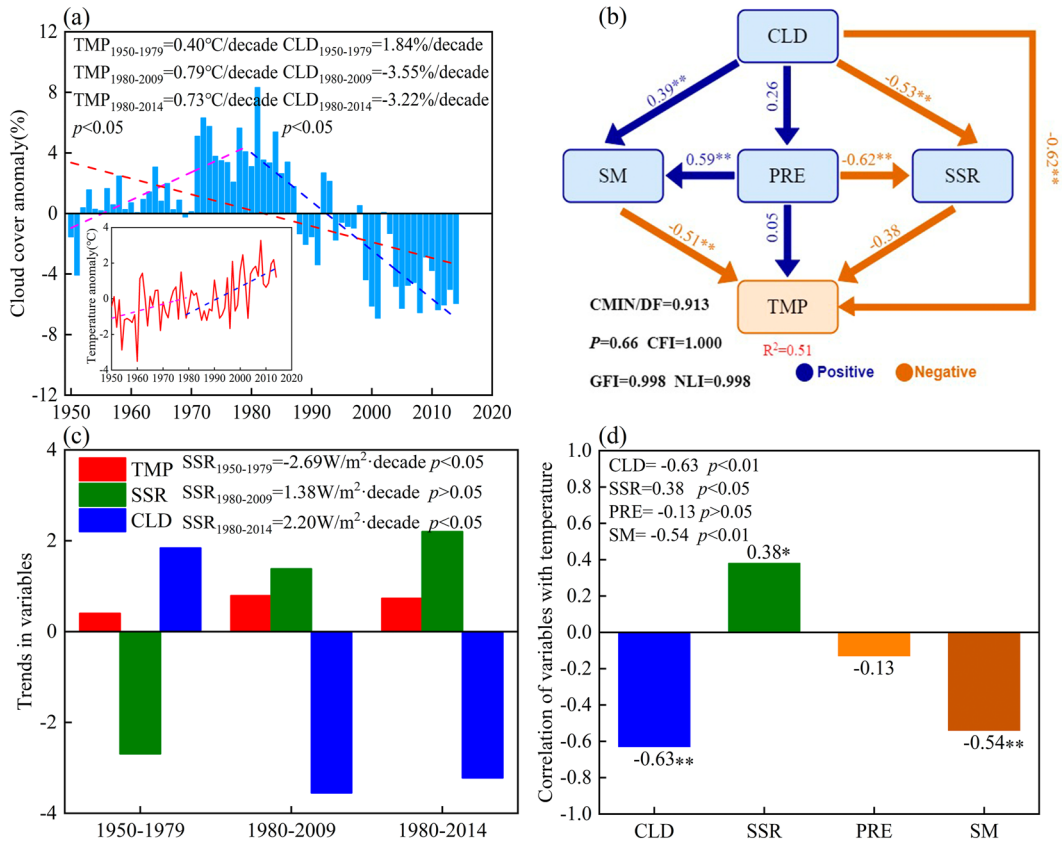

Figure 3. Attributions of potential factors to spring warming in Central Asia (CA). (a) Spring cloud cover anomalies in CA from 1950 to 2014; (b) Structural equation modeling of spring temperature and influencing factors; (c) Spring temperature, downward solar shortwave radiation flux and cloud cover trend of change in CA from 1950 to 2014; (d) The correlation between spring temperature and factors in CA from 1980 to 2014. Note: ** and * represent significance at the levels of 1% and 5%, respectively.

other variables had a weak relationship with spring temperature (Figure 3d). Spatially, temperature is negatively correlated with CLD in 93.54% of the regions (Figure S4 in Supporting Information S1).

Figure 3a shows that the temperature experienced an overall upward trend from 1950 to 2014. However, the warming rate from 1980 to 2014 (0.73°C/decade) is higher than that from 1950 to 1979 (0.40°C/decade), indicating a faster warming trend in CA during 1980–2014. Additionally, CLD shows an opposite trend during those two periods, with a decreasing trend in CLD from 1980 to 2014 (−3.22%/decade), and an increasing trend in CLD from 1950 to 1979 (1.84%/decade). These results suggest a positive feedback effect of CLD decrease on the TMP trend during 1980–2014. We also observed an increasing trend in spring SSR from 1980 to 2014 (2.20 W/m^2 · decade), and a decreasing trend in SSR from 1950 to 1979 (−2.69 W/m^2 · decade). Besides, the significantly negative correlation between CLD and SSR ($R = -0.68$, $p < 0.01$) suggests that the decrease in CLD led to an increase in SSR, resulting in a warming effect on temperature. Therefore, the rapid increase in spring temperatures from 1980 to 2014 was driven by the decrease in CLD. The SEM was further used to quantify the total impact of factors on temperature. The constructed SEM were robust, with CMIN/DF and RMSAE values of 0.193 and 0.001, respectively. The results show that CLD is the most important influencing factor in spring temperature, followed by SM, SSR, and PRE (Figure 3b). Besides, the contributions of these four variables to temperature were CLD (40.79%) > SM (33.44%) > SSR (24.72%) > PRE (1.05%). Therefore, CLD has the largest contribution to spring temperature and is the main factor affecting spring temperature in CA.

3.3. Response of SLP and VV to Temperature

The formation of clouds highly depends on the SLP and VV changes. High-pressure areas are usually not conducive to cloud formation, since the SLP leads to downward movement of air (i.e., positive VV). To further

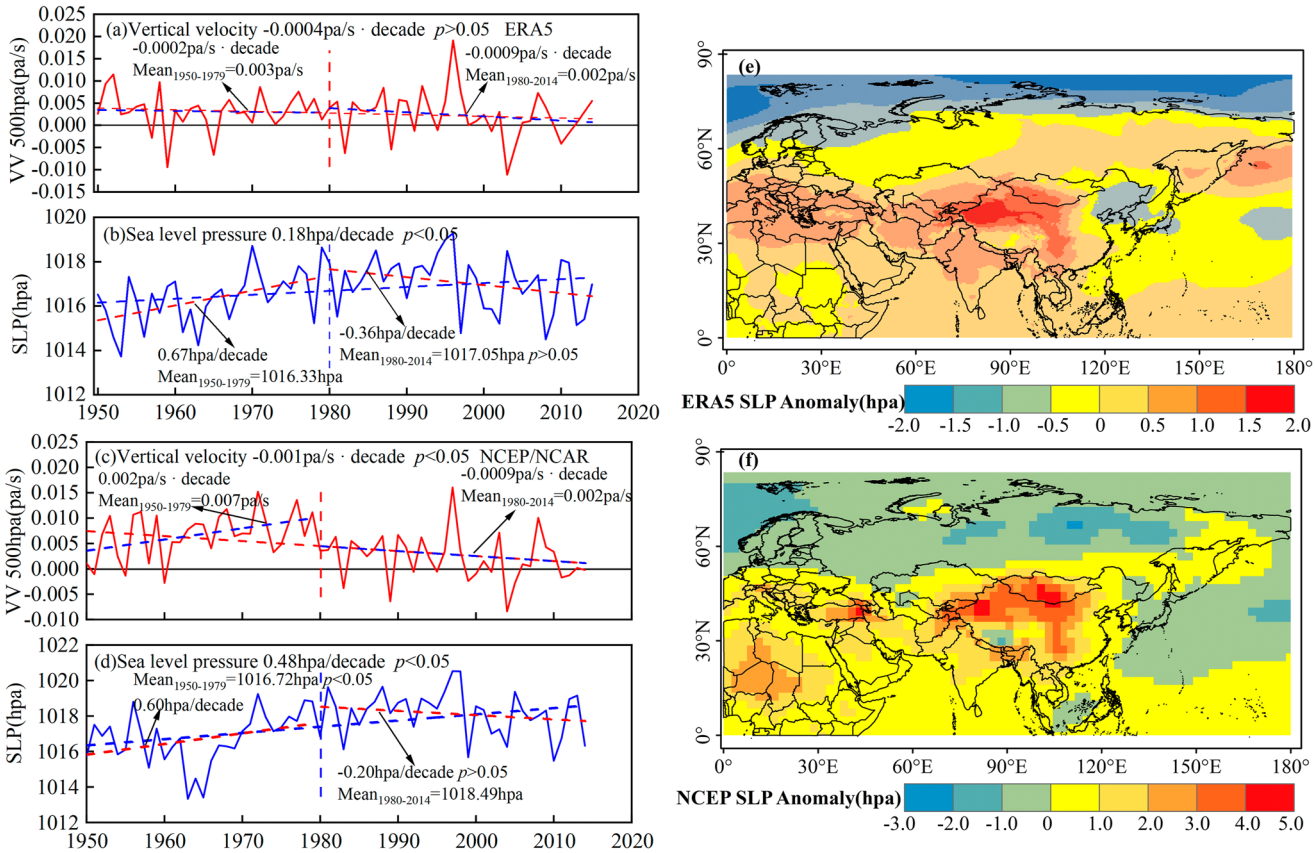

Figure 4. The influence of sea level pressure (SLP) and vertical velocity (VV) on cloud cover changes (a, b) Temporal changes in VV and SLP during 1950–2014, respectively, based on ERA5 data sets; (c, d) Same as (a, b), but for the National Centers for Environmental Prediction (NCEP)/National Center for Atmospheric Research (NCAR) data sets. (e) Difference between 1980–2014 and 1950–1979 SLP from ERA5. (f) Difference between 1980–2014 and 1950–1979 SLP from NCEP/NCAR. VV includes areas of upward movement/rise (negative value) and downward movement/sink (positive value).

investigate the relations between SLP, VV, and CLD, we calculated the variations of both SLP and VV during 1950–2014.

The SLP from ERA5 shows an overall increasing trend from 1950 to 2014, with a higher SLP value of 1,017.05 hPa during 1980–2014 than the value of 1,016.33 hPa during 1950–1979 (Figure 4b). The result is similar to the NCEP data sets in that the SLP was strengthened during 1980–2014 (i.e., 1,018.15 vs. 1,016.72 hPa). This result was supported by the positive VV values during all the above two periods, suggesting a persistent moving downward of VV. Spatially, the SLP difference between the two time periods (1980–2014 minus 1950–1979) shows positive values covering the whole CA, with a hotspot in Xinjiang Province, China (Figures 4e and 4f). The results above indicate that the increased SLP in CA during 1980–2014 impeded the formation of clouds in CA.

4. Discussion and Conclusions

The CA experienced a rapid temperature rise over the past decades, which is higher than the global land. This rapid warming trend will continue till the end of this century, which is confirmed by the CMIP model simulations. This result is supported by previous studies, which are based on other data sets, such as the Japanese 55-year reanalysis (JRA55), and the database of the Goddard Institute for Space Studies (GISS) (F. Chen et al., 2009; Z. Chen et al., 2023). Additionally, the raid annual warming trend was mainly dominated by accelerated spring warming with a value of 0.73°C/decade. On the contrary, the winter was widely reported as the fastest rate of warming among all seasons in other regions, such as western North America, northern Europe, and China (Huang et al., 2005; B. Li et al., 2012; Peng et al., 2019; Trenberth & Josey, 2007). However, we found that temperature in the winter, summer, and autumn in CA was slow and leveling off, suggesting that spring warming has become the main cause of rising temperature in CA (Figure 2c).

We found that the spring CLD in CA decreased significantly from 1980 to 2014, with a 40.79% warming contribution to temperature rise in CA. This result suggests a high dependence of CA warming on CLD, evidenced by the fact that CLD decrease acted as a positive feedback on temperature rise. Our findings are consistent with previous studies that a negative relationship between CLD variations and the rate of warming was reported at the global scale (Warren et al., 2007), or at the continental/regional scales, such as Eurasia (Matuszko et al., 2022), and China (Jiang et al., 2022). For example, the CLD is an important factor in regulating temperature changes over Eurasia, and the decrease in CLD is the main reason for the increase in land surface temperature (Ma et al., 2021; Tang & Leng, 2012). As a factor affecting temperature, CLD has important implications for climate change. Therefore, studying the influence of CLD on temperature can deepen our understanding of temperature evolution in CA.

The changes in SLP can influence the increase or decrease of surface temperatures (Gillett et al., 2003; Juzhang et al., 2003). This study found a rising trend in SLP from 1950 to 2014 in CA, which is consistent with previous studies (Wu et al., 2010; Y. Zhang et al., 2012). SLP in CA exhibits positive anomalies, accompanied by the sinking of VV, which hinders cloud formation. The CLD decrease allows more solar radiation to reach the land surface, hence, leading to a rapid increase in temperatures during the spring season in CA. The SLP changes in CA are mainly influenced by the North Atlantic Oscillation and the Siberian High according to previous studies (Gong et al., 2001; F. Zhou et al., 2023). This suggests that changes in SLP are both influenced by regional factors and closely linked to changes in atmospheric circulation patterns.

This study mainly focused on discussing the factors causing rapid warming in CA, such as CLD, SLP, and VV, but it is also necessary to consider the impact of other factors on CA warming, such as anthropogenic activities, atmospheric circulation, changes in land use/land cover, and aerosol emissions. Therefore, comprehensively assessing the impacts of various factors on warming in the Central Asian region will be beneficial for us to gain a deeper understanding of temperature changes in CA.

Conflict of Interest

The authors declare no conflicts of interest relevant to this study.

Data Availability Statement

CRU data is downloaded from https://crudata.uea.ac.uk/cru/data/hrg/cru_ts_4.06/cruts.2205201912.v4.06/; CMIP6 temperature from https://esgf-node.llnl.gov/search/cmip6/; NCEP reanalysis data sets from http://poles.tpdc.ac.cn/zh-hans/data/2793ba69-7122-4a62-876b-647a1a50a121/; ERA5 data can be download from https://cds.climate.copernicus.eu/cdsapp#!/home.

Acknowledgments
This research was financially supported by the National Natural Science Foundation of China (Grant 42105118 and 42161024), the Key Laboratory Project of Xinjiang Uygur Autonomous Region, China (Grant 2023D04072), the High-end Foreign Expert Recruitment Program from the Ministry of Science and Technology of China (Grant G2022045012L), and the Project for Cultivating High-Level Talent of Xinjiang Institute of Ecology and Geography, Chinese Academy of Sciences (Grants E1500103, E3150101, and E3150102).

References

Bai, J., Shi, H., Yu, Q., Xie, Z., Li, L., Luo, G., et al. (2019). Satellite-observed vegetation stability in response to changes in climate and total water storage in Central Asia. *Science of the Total Environment*, *659*, 862–871. https://doi.org/10.1016/j.scitotenv.2018.12.418

Barrios, S., Ouattara, B., & Strobl, E. (2008). The impact of climatic change on agricultural production: Is it different for Africa? *Food Policy*, *33*(4), 287–298. https://doi.org/10.1016/j.foodpol.2008.01.003

Bednorz, E., Kaczmarek, D., & Dudlik, P. (2016). Atmospheric conditions governing anomalies of the summer and winter cloudiness in Spitsbergen. *Theoretical and Applied Climatology*, *123*(1–2), 1–10. https://doi.org/10.1007/s00704-014-1326-5

Bothe, O., Fraedrich, K., & Zhu, X. (2012). Precipitation climate of Central Asia and the large-scale atmospheric circulation. *Theoretical and Applied Climatology*, *108*(3–4), 345–354. https://doi.org/10.1007/s00704-011-0537-2

Chen, F., Wang, J., Jin, L., Zhang, Q., Li, J., & Chen, J. (2009). Rapid warming in mid-latitude central Asia for the past 100 years. *Frontiers of Earth Science in China*, *3*(1), 42–50. https://doi.org/10.1007/s11707-009-0013-9

Chen, F., Yuan, Y., Wei, W., Wang, L., Yu, S., Zhang, R., et al. (2012). Tree ring density-based summer temperature reconstruction for Zajsan Lake area, East Kazakhstan. *International Journal of Climatology*, *32*(7), 1089–1097. https://doi.org/10.1002/joc.2327

Chen, G., Wang, W. C., Bao, Q., & Li, J. (2022). Evaluation of simulated cloud diurnal variation in CMIP6 climate models. *Journal of Geophysical Research: Atmospheres*, *127*(6), e2021JD036422. https://doi.org/10.1029/2021jd036422

Chen, T., Bao, A., Jiapaer, G., Guo, H., Zheng, G., Jiang, L., et al. (2019). Disentangling the relative impacts of climate change and human activities on arid and semiarid grasslands in Central Asia during 1982–2015. *Science of the Total Environment*, *653*, 1311–1325. https://doi.org/10.1016/j.scitotenv.2018.11.058

Chen, Z., Wu, R., Zhao, Y., & Wang, Z. (2023). Roles of dynamic and thermodynamic effects in seasonal mean surface air temperature trends over Central Asia during 1979–2018. *Climate Dynamics*, *60*(7), 2331–2342. https://doi.org/10.1007/s00382-022-06457-0

Deng, H., & Chen, Y. (2017). Influences of recent climate change and human activities on water storage variations in Central Asia. *Journal of Hydrology*, *544*, 46–57. https://doi.org/10.1016/j.jhydrol.2016.11.006

Diffenbaugh, N. S., & Burke, M. (2019). Global warming has increased global economic inequality. *Proceedings of the National Academy of Sciences of the United States of America*, *116*(20), 9808–9813. https://doi.org/10.1073/pnas.1816020116

Dong, D., Huang, G., Qu, X., Tao, W., & Fan, G. (2015). Temperature trend–altitude relationship in China during 1963–2012. *Theoretical and Applied Climatology*, *122*(1), 285–294. https://doi.org/10.1007/s00704-014-1286-9

Duveiller, G., Hooker, J., & Cescatti, A. (2018). The mark of vegetation change on Earth's surface energy balance. *Nature Communications*, *9*(1), 679. https://doi.org/10.1038/s41467-017-02810-8

Fan, X., Duan, Q., Shen, C., Wu, Y., & Xing, C. (2020). Global surface air temperatures in CMIP6: Historical performance and future changes. *Environmental Research Letters*, *15*(10), 104056. 104014. https://doi.org/10.1088/1748-9326/abb051

Gidden, M. J., Riahi, K., Smith, S. J., Fujimori, S., Luderer, G., Kriegler, E., et al. (2019). Global emissions pathways under different socio-economic scenarios for use in CMIP6: A dataset of harmonized emissions trajectories through the end of the century. *Geoscientific Model Development*, *12*(4), 1443–1475. https://doi.org/10.5194/gmd-12-1443-2019

Gillett, N. P., Zwiers, F. W., Weaver, A. J., & Stott, P. A. (2003). Detection of human influence on sea-level pressure. *Nature*, *422*(6929), 292–294. https://doi.org/10.1038/nature01487

Gong, D.-Y., & Ho, C.-H. (2002). The Siberian High and climate change over middle to high latitude Asia. *Theoretical and Applied Climatology*, *72*(1–2), 1–9. https://doi.org/10.1007/s007040200008

Gong, D.-Y., Wang, S. W., & Zhu, J. H. (2001). East Asian winter monsoon and Arctic oscillation. *Geophysical Research Letters*, *28*(10), 2073–2076. https://doi.org/10.1029/2000gl012311

Grace, J. B. (2006). *Structural equation modeling and natural systems*. Cambridge University Press.

Grant, L. D., van den Heever, S. C., Haddad, Z. S., Bukowski, J., Marinescu, P. J., Storer, R. L., et al. (2022). A linear relationship between vertical velocity and condensation processes in deep convection. *Journal of the Atmospheric Sciences*, *79*(2), 449–466. https://doi.org/10.1175/jas-d-21-0035.1

Guo, A., Yang, J., Sun, W., Xiao, X., Cecilia, J. X., Jin, C., & Li, X. (2020). Impact of urban morphology and landscape characteristics on spatiotemporal heterogeneity of land surface temperature. *Sustainable Cities and Society*, *63*, 102443. https://doi.org/10.1016/j.scs.2020.102443

Hájek, M., Zimmermannová, J., Helman, K., & Rozenský, L. (2019). Analysis of carbon tax efficiency in energy industries of selected EU countries. *Energy Policy*, *134*, 110955. https://doi.org/10.1016/j.enpol.2019.110955

Hansen, J., Ruedy, R., Sato, M., & Lo, K. (2010). Global surface temperature change. *Reviews of Geophysics*, *48*(4), 1–29. https://doi.org/10.1029/2010RG000345

Hansen, J., Sato, M., Kharecha, P., & Von Schuckmann, K. (2011). Earth's energy imbalance and implications. *Atmospheric Chemistry and Physics*, *11*(24), 13421–13449. https://doi.org/10.5194/acp-11-13421-2011

Harris, I., Osborn, T. J., Jones, P., & Lister, D. (2020). Version 4 of the CRU TS monthly high-resolution gridded multivariate climate dataset. *Scientific Data*, *7*(1), 109. https://doi.org/10.1038/s41597-020-0453-3

He, M., Piao, S., Huntingford, C., Xu, H., Wang, X., Bastos, A., et al. (2022). Amplified warming from physiological responses to carbon dioxide reduces the potential of vegetation for climate change mitigation. *Communications Earth & Environment*, *3*(1), 160. https://doi.org/10.1038/s43247-022-00489-4

Hu, X., Sejas, S. A., Cai, M., Taylor, P. C., Deng, Y., & Yang, S. (2019). Decadal evolution of the surface energy budget during the fast warming and global warming hiatus periods in the ERA-interim. *Climate Dynamics*, *52*(3–4), 2005–2016. https://doi.org/10.1007/s00382-018-4232-1

Hu, Z., Chen, D., Chen, X., Zhou, Q., Peng, Y., Li, J., & Sang, Y. (2022). CCHZ-DISO: A timely new assessment system for data quality or model performance from Da Dao Zhi Jian. *Geophysical Research Letters*, *49*(23), e2022GL100681. https://doi.org/10.1029/2022gl100681

Hu, Z., Zhang, C., Hu, Q., & Tian, H. (2014). Temperature changes in Central Asia from 1979 to 2011 based on multiple datasets. *Journal of Climate*, *27*(3), 1143–1167. https://doi.org/10.1175/jcli-d-13-00064.1

Huang, M., Peng, G., Leslie, L. M., Shao, X., & Sha, W. (2005). Seasonal and regional temperature changes in China over the 50 year period 1951–2000. *Meteorology and Atmospheric Physics*, *89*(1–4), 105–115. https://doi.org/10.1007/s00703-005-0124-0

Jiang, S., Zhao, C., & Xia, Y. (2022). Distinct response of near surface air temperature to clouds in North China. *Atmospheric Science Letters*, *23*(12), e1128. https://doi.org/10.1002/asl.1128

Jing, C.-Q., & Li, L.-H. (2016). Simulating the energy and water fluxes from two alkaline desert ecosystems over Central Asia. *Advances in Meteorology*, *2016*, 1–13. https://doi.org/10.1155/2016/4849525

Juzhang, R., Jianhua, J., & Gang, Z. (2003). Relation between the winter surface air temperature fields in Asia and the Northern Hemisphere sea level pressure. *Climatic and Environmental Research*, *8*(4), 436–441. (in Chinese).

Li, B., Chen, Y., & Shi, X. (2012). Why does the temperature rise faster in the arid region of northwest China? *Journal of Geophysical Research*, *117*, D16115. https://doi.org/10.1029/2012jd017953

Li, H., & Fan, K. (2022). Dominant patterns of winter surface air temperature over Central Asia and their connection with atmospheric circulation. *Atmospheric and Oceanic Science Letters*, *15*(6), 100210. https://doi.org/10.1016/j.aosl.2022.100210

Li, Q., Chen, Y., Shen, Y., Li, X., & Xu, J. (2011). Spatial and temporal trends of climate change in Xinjiang, China. *Journal of Geographical Sciences*, *21*(6), 1007–1018. https://doi.org/10.1007/s11442-011-0896-8

Ma, Q., You, Q., Ma, Y., Cao, Y., Zhang, J., Niu, M., & Zhang, Y. (2021). Changes in cloud amount over the Tibetan Plateau and impacts of large-scale circulation. *Atmospheric Research*, *249*, 105332. https://doi.org/10.1016/j.atmosres.2020.105332

Marshall, J., Scott, J. R., Armour, K. C., Campin, J.-M., Kelley, M., & Romanou, A. (2015). The ocean's role in the transient response of climate to abrupt greenhouse gas forcing. *Climate Dynamics*, *44*(7–8), 2287–2299. https://doi.org/10.1007/s00382-014-2308-0

Martens, B., Miralles, D. G., Lievens, H., Van Der Schalie, R., De Jeu, R. A., Fernández-Prieto, D., et al. (2017). GLEAM v3: Satellite-based land evaporation and root-zone soil moisture. *Geoscientific Model Development*, *10*(5), 1903–1925. https://doi.org/10.5194/gmd-10-1903-2017

Matuszko, D., Bartoszek, K., & Soroka, J. (2022). Long-term variability of cloud cover in Poland (1971–2020). *Atmospheric Research*, *268*, 106028. https://doi.org/10.1016/j.atmosres.2022.106028

Mori, N., Takemi, T., Tachikawa, Y., Tatano, H., Nakakita, E., Tanaka, T., et al. (2021). Recent nationwide climate change impact assessments of natural hazards in Japan and East Asia. *Weather and Climate Extremes*, *32*(2), 100309. https://doi.org/10.1016/j.wace.2021.100309

Peng, D., Zhou, T., Zhang, L., & Zou, L. (2019). Detecting human influence on the temperature changes in Central Asia. *Climate Dynamics*, *53*(7), 4553–4568. https://doi.org/10.1007/s00382-019-04804-2

Revadekar, J., Hameed, S., Collins, D., Manton, M., Sheikh, M., Borgaonkar, H., et al. (2013). Impact of altitude and latitude on changes in temperature extremes over South Asia during 1971–2000. *International Journal of Climatology*, *33*(1), 199–209. https://doi.org/10.1002/joc.3418

Shouguo, D., Guangyu, S., & Chunsheng, Z. (2004). Analyzing global trends of different cloud types and their potential impacts on climate by using the ISCCP D2 dataset. *Chinese Science Bulletin*, *49*(12), 1301–1306. https://doi.org/10.1360/03wd0614

Stocker, T. F., Qin, D., Plattner, G. K., Tignor, M. M. B., Allen, S. K., Boschung, J., et al. (2014). Climate change 2013: The physical science basis. Contribution of Working Group I to the fifth assessment report of IPCC the Intergovernmental Panel on Climate Change (Vol. *18*, (No. 2), pp. 95–123).

Sun, B., & Wang, H. (2014). Moisture sources of semiarid grassland in China using the Lagrangian particle model FLEXPART. *Journal of Climate*, *27*(6), 2457–2474. https://doi.org/10.1175/jcli-d-13-00517.1

Tang, Q., & Leng, G. (2012). Damped summer warming accompanied with cloud cover increase over Eurasia from 1982 to 2009. *Environmental Research Letters*, *7*(1), 014004. https://doi.org/10.1088/1748-9326/7/1/014004

Thompson, D. W., & Wallace, J. M. (2000). Annular modes in the extratropical circulation. Part I: Month-to-month variability. *Journal of Climate*, *13*(5), 1000–1016. https://doi.org/10.1175/1520-0442(2000)013<1000:amitec>2.0.co;2

Tian-Jun, Z., Zi-Ming, C., Xiao-Long, C., Meng, Z., Jie, J., & Shuai, H. (2021). Interpreting IPCC AR6: Future global climate based on projection under scenarios and on near-term information. *Advances in Climate Change Research*, *17*(6), 652.

Trenberth, K. E., & Josey, S. A. (2007). Observations: Surface and atmospheric climate change. In *Climate change 2007: The physical science basis. Contribution of Working Group I to the fourth assessment report of the Intergovernmental Panel on Climate Change*.

Warren, S. G., Eastman, R. M., & Hahn, C. J. (2007). A survey of changes in cloud cover and cloud types over land from surface observations, 1971–96. *Journal of Climate*, *20*(4), 717–738. https://doi.org/10.1175/jcli4031.1

Wu, R., Wen, Z., Yang, S., & Li, Y. (2010). An interdecadal change in southern China summer rainfall around 1992/93. *Journal of Climate*, *23*(9), 2389–2403. https://doi.org/10.1175/2009jcli3336.1

Xu, T., Shao, H., & Zhang, C. (2015). Temporal pattern analysis of air temperature change in Central Asia during 1980–2011. *Arid Land Geography*, *38*(1), 25–35.

Zhang, Q., Liu, B., Li, S., & Zhou, T. (2023). Understanding models' global sea surface temperature bias in mean state: From CMIP5 to CMIP6. *Geophysical Research Letters*, *50*(4), e2022GL100888. https://doi.org/10.1029/2022gl100888

Zhang, Y., Ding, Y., & Li, Q. (2012). A climatology of extratropical cyclones over East Asia during 1958–2001. *Acta Meteorologica Sinica*, *26*(3), 261–277. https://doi.org/10.1007/s13351-012-0301-2

Zheng, H., Miao, C., Wu, J., Lei, X., Liao, W., & Li, H. (2019). Temporal and spatial variations in water discharge and sediment load on the Loess Plateau, China: A high-density study. *Science of the Total Environment*, *666*(MAY 20), 875–886. https://doi.org/10.1016/j.scitotenv.2019.02.246

Zhou, C., Zelinka, M. D., & Klein, S. A. (2016). Impact of decadal cloud variations on the Earth's energy budget. *Nature Geoscience*, *9*(12), 871–874. https://doi.org/10.1038/ngeo2828

Zhou, F., Shi, J., Liu, M.-H., & Ren, H.-C. (2023). Linkage between the NAO and Siberian high events on the intraseasonal timescale. *Atmospheric Research*, *281*, 106478. https://doi.org/10.1016/j.atmosres.2022.106478